Dear Author

Please use this PDF proof to check the layout of your article. If you would like any changes to be made to the layout, you can leave instructions in the online proofing interface. Making your changes directly in the online proofing interface is the quickest, easiest way to correct and submit your proof. Please note that changes made to the article in the online proofing interface will be added to the article before publication, but are not reflected in this PDF proof.

If you would prefer to submit your corrections by annotating the PDF proof, please download and submit an annotatable PDF proof by clicking here and you'll be redirected to our PDF Proofing system.

INTERNATIONAL JOURNAL OF HYDROGEN ENERGY XXX (XXXX) XXX

Available online at www.sciencedirect.com

ScienceDirect

journal homepage: www.elsevier.com/locate/he

Modelling of the ethanol steam reforming over Rh-Pd/CeO_2 catalytic wall reactors

Alejandro Cifuentes [a,b], Ricardo Torres [b,**], Jordi Llorca [a,*]

[a] Institute of Energy Technologies, Department of Chemical Engineering and Barcelona Research Center in Multiscale Science and Engineering, Universitat Politècnica de Catalunya, EEBE, Eduard Maristany 10-14, 08019, Barcelona, Spain

[b] Department of Fluid Mechanics, Universitat Politècnica de Catalunya, EEBE, Eduard Maristany 10-14, 08019, Barcelona, Spain

HIGHLIGHTS

- Ethanol steam reforming has been modelled with a 3D non-isothermal model.
- EtOH decomposition, water gas shift and CH_4 steam reforming have been considered.
- Honeycombs loaded with Rh-Pd/CeO_2 catalyst have been modelled at S/C = 3.
- A maximum H_2 yield of 80% is achieved at 1150 K and 4 bar.

ARTICLE INFO

Article history:
Received 26 July 2019
Received in revised form
1 November 2019
Accepted 6 November 2019
Available online xxx

Keywords:
Hydrogen
CFD model
Ethanol steam reforming
Catalytic wall reactor
Ceria-based catalyst
Structured catalyst

ABSTRACT

Existing literature data have been used to model the steam reforming of ethanol on catalytic honeycombs coated with Rh-Pd/CeO_2, which have shown an excellent performance and robustness for the production of hydrogen under realistic conditions. In this article, a fully 3D non-isothermal model is presented, where the reactions of ethanol decomposition, water gas shift, and methane steam reforming have been modelled under different operational pressures (1–10 bar) and temperatures (500–1200 K) at a steam to carbon ratio of S/C = 3 and a space time of W/F between $2{\cdot}10^{-3}$ and 3 kg h L_{liq}^{-1}. According to the modelling results, a maximum hydrogen yield of 80% is achieved at a working temperature of 1150 K and a pressure of 4 bar at S/C = 3.

Introduction

The demand for clean and renewable energy is increasing because of stringent environmental and political constraints. In this context, hydrogen is emerging as a natural choice because it is an excellent energy carrier and represents the final objective of a decarbonized society. In addition, fuel cells can be used to produce electricity and heat from hydrogen with remarkable efficiency and flexibility. As a renewable substance, hydrogen cannot only be used as a clean fuel but

* Corresponding author. Universitat Politècnica de Catalunya Eduard Maristany, 10-14 08019, Barcelona, Spain.
** Corresponding author.
E-mail addresses: ricardo.torres@upc.edu (R. Torres), jordi.llorca@upc.edu (J. Llorca).

https://doi.org/10.1016/j.ijhydene.2019.11.034

also as a feedstock for important chemical production, such as ammonia and methanol. The production of hydrogen from natural gas and naphtha by catalytic reforming is a well-established commercial process, but hydrogen can be also produced catalytically from a variety of other sources, including other hydrocarbons, various types of alcohols and bio-alcohols, ammonia, etc. as well as photocatalytically from water and organic compounds [1,2]. Advances in catalytic reactor technologies are essential for process intensification in the production of hydrogen, particularly for on-site and/or on-board applications intended to feed fuel cells [3]. Catalytic wall reactors, where a thin layer of catalyst is deposited on the walls of a regular substrate, is one of the most used methods to immobilize a catalyst and to improve mass and heat transfer with low pressure drop for practical application.

In this work, we focus on the modelling of catalytic honeycombs for the steam reforming of ethanol (ESR). Ethanol is a renewable fuel that is widely produced by biomass fermentation and its use to produce hydrogen has been widely reported and reviewed [4–7]. Given the worldwide availability of bioethanol, high hydrogen content, safe transport and manipulation and low cost, considerable effort has been devoted to obtain highly active and robust catalysts for operating in real environments. In that sense, we have reported previously the excellent performance of the bimetallic Rh-Pd system supported on cerium dioxide and studied in detail its performance in the ESR reaction, both in powder form [8–12] as well as the active phase in catalytic wall reactors [13,14], catalytic membrane reactors equipped with highly selective metallic membranes [15,16] and microreactors [17]. Here we extend these studies by developing a CFD model for cordierite honeycombs coated with Rh-Pd/CeO_2 in the ESR reaction based on our previous experimental data to better understand their behaviour and to simulate and optimize operation parameters.

Methods

Reformer configuration

A fully detailed description of the catalyst preparation, characterization, reaction tests and the experimental set-up can be found in Ref. [13]. Briefly, a conventional 400 cpsi (cells per square inch) cordierite honeycomb (Corning Inc.) with 1.8 cm diameter and length was coated with cerium dioxide by the washcoating method. Then, the noble metals (0.5 wt%Rh – 0.5 wt% Pd) were added by incipient wetness impregnation. The total mass of the Rh-Pd/CeO2 catalyst deposited on the honeycomb was 250 mg and the catalyst layer thickness was about 5–6 μm. The catalytic honeycomb was implemented in a tubular stainless-steel reactor, which was disposed inside an electric furnace with a PID electronic controller. The liquid feed mixture of ethanol and water (steam to carbon ratio of 3) was injected into the reactor with an HPLC pump (no carrier gas was used). A back-pressure regulator was implemented after the reactor outlet. Finally, a condenser was added to collect the condensable components from the reactor, the gas flow stream was measured with a bubble soap meter, and a micro GC (Agilent 3000 A) was used to measure online the concentration of the different gas species.

CFD model

A 3D non-isothermal model was developed using CFD methods to simulate the catalytic honeycomb for hydrogen production described above. Taking advantage of the symmetry of the honeycomb, only 1/8 part of it was modelled (Fig. 1). The commercial CFD software COMSOL Multiphysics 5.4 was used with the finite-element method for solving the governing equations. In order to obtain the best convergence and reliable results, a fully coupled solution approach (a single large system of equations that solves every physics coupling within a single iteration) was carried out with the direct solver PARDISO. The hardware configuration was an 8 core CPU at 4.7 GHz (Intel i9 9900k) with 32 GB RAM memory at 3000 MHz. The following assumptions for the CFD model were considered [18–30]: (i) ideal gas behaviour and Newtonian flow, (ii) steady state conditions, (iii) steam acts like a solvent for diffusion transport calculations, (iv) inertial term on the Navier Stokes equation is neglected, (v) thermal viscous dissipation of the fluid flow is neglected, (vi) reactions take place only at the surface of the catalyst, and (vii) conductive heat transfer within the catalyst layer is similar to that of the cordierite support. The temperature of the external wall of the monolith was fixed as a boundary condition to simulate

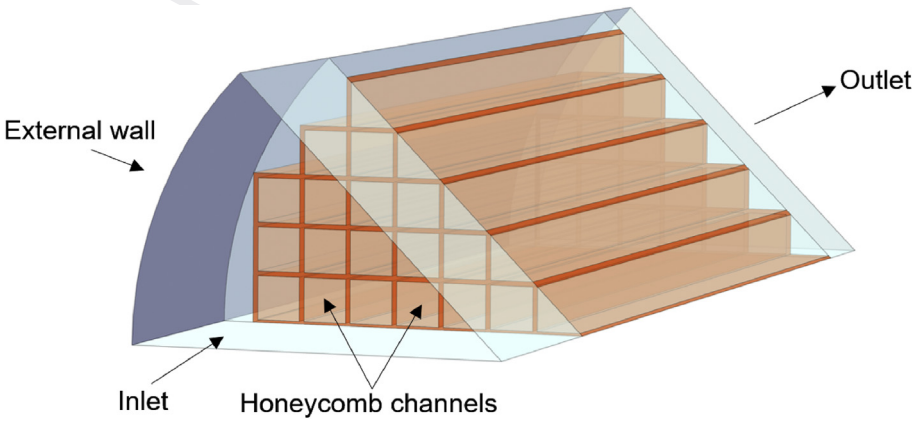

Fig. 1 – Geometry of the model.

Please cite this article as: Cifuentes A et al., Modelling of the ethanol steam reforming over Rh-Pd/CeO_2 catalytic wall reactors, International Journal of Hydrogen Energy, https://doi.org/10.1016/j.ijhydene.2019.11.034

experiments, which were carried out with the catalytic reactor inside an electrical furnace, as explained in Reformer configuration.

Governing equations

The governing equations of the model are: (i) continuity equation (Eq. (1)), (ii) momentum balance (Navier-Stokes, Eq. 2), (iii) energy balance equation (Eq. (3)), and (iv) conservation equation (Eq. (4)).

$$\nabla(\rho_f \cdot u) = 0 \tag{1}$$

$$0 = -\nabla p + \nabla\cdot(\mu(\nabla u + (\nabla u)^T) - \frac{2}{3}\mu(\nabla\cdot u)I) + F \tag{2}$$

$$\rho_f C_p u\cdot\nabla T + \nabla\cdot(-k_{con}\nabla T) = Q + Q_r \tag{3}$$

$$\nabla\cdot(-D_i\nabla c_i + uc_i) = R_i \tag{4}$$

According to the literature [8,13,17], ethanol is first decomposed into hydrogen, methane and carbon monoxide on the Rh-Pd/CeO2 catalysts at low temperature (Eq. (5)), followed by the water gas shift reaction (WGS, Eq. (6)) [8,31] and methane reforming at high temperature (MSR, Eq. (7)) [32].

$$C_2H_5OH(g) \rightarrow CH_4(g) + CO(g) + H_2(g)\left(\Delta H_{298\ K} = 49.0\ kJ\ mol^{-1}\right) \tag{5}$$

$$CO(g) + H_2O(g) \rightleftarrows CO_2(g) + H_2(g)\left(\Delta H_{298\ K} = -41.2\ kJ\ mol^{-1}\right) \tag{6}$$

$$CH_4(g) + 2H_2O(g) \rightleftarrows CO_2(g) + 4H_2(g)\left(\Delta H_{298\ K} = 165.1\ kJ\ mol^{-1}\right) \tag{7}$$

As reported in Refs. [23,24], due to the involved significant computational efforts to build a CFD model, the reactions rates (Eqs. (8)–(10)) were modelled in a simplified way in order to keep the equations numerically tractable:

$$r_5 = k_5\cdot C_{C_2H_5OH} \tag{8}$$

$$r_6 = k_6\cdot C_{CO}\cdot C_{H_2O} - \frac{k_6\cdot C_{CO_2}\cdot C_{H_2}}{K_6} \tag{9}$$

$$r_7 = k_7\cdot C_{CH_4}\cdot C_{H_2O}^2 - \frac{k_7\cdot C_{CO_2}\cdot C_{H_2}^4}{K_7} \tag{10}$$

$$k_j = k_{\infty,j}\cdot e^{\frac{-Ea_j}{R\cdot T}} \tag{11}$$

where r_5, r_6 and r_7 correspond to the reactions rates (in mol m^{-2} s^{-1}) of ethanol decomposition, water gas shift and methane reforming, respectively. $C_{C_2H_5OH}$, C_{CO}, C_{CO_2}, C_{H_2O}, C_{H_2} and C_{CH_4} are the molar concentrations of each species. k_5, k_6, k_7 are the rate constants calculated from Arrhenius equation (Eq. (11)).

The equilibrium constants (Kj) were calculated from the Gibbs free energy of the reaction (Eq. (12)).

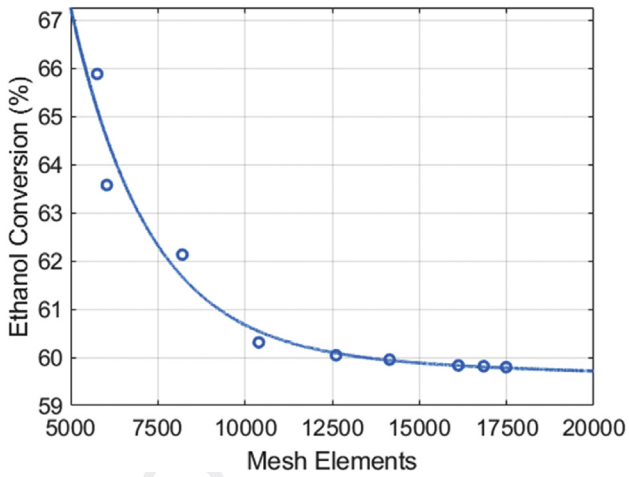

Fig. 2 – Effect of mesh element number in CFD simulation on ethanol conversion (6 bar, 700 K, S/C = 3, 55 μL_{liq}/min).

$$K_j = e^{\frac{-\Delta G_r^\circ}{RT}}\prod_{species}\left(\frac{C_{total}\cdot p^\circ}{p}\right)^{\gamma_{species\ i}} \tag{12}$$

Where ΔG_r° is the Gibbs free energy of the reaction (including formation terms). In order to obtain the best accuracy, the enthalpy and entropy of the reaction were calculated from the standard enthalpy formation and absolute entropy of each species referred to a given temperature. Polynomial approximations of thermodynamic and transport properties were modelled for each species (NASA coefficients) [33].

Boundary conditions and post-processing definitions

The following boundary conditions were taken into account:

- Inlet of the reformer: $n\cdot(J_i + uc_i) = n\cdot(uc_{0,i})$, $T = T_{in}$, $-\int_{\partial\Omega}\rho(u\cdot n)\,dS = m$.
- Catalytic walls: $-n\cdot J_i = R_i$, $-n\cdot(-k_{con}\nabla T) = Q$, $u = 0$.
- External wall: $-n\cdot J_i = 0$, $T = T_0$, $u = 0$.
- Symmetry: $-n\cdot J_i = 0$, $-n\cdot q = 0$, $u\cdot n = 0$, $(\mu(\nabla u + (\nabla u)^T)n) - ((\mu(\nabla u + (\nabla u)^T)n)\cdot n)n = 0$.
- Outlet of the reformer: $n\cdot D_i\nabla c_i = 0$, $-n\cdot q = 0$, $[-pI + (\mu(\nabla u + (\nabla u)^T)n)]n = 0$.

The following definitions were used on the post-processing:

- Ethanol conversion:

Table 1 – Estimated parameters for reaction rates.

Reaction j	k_{∞}, j	E_a, j
Ethanol Decomposition Eq. (8)	4.3864 m mg_{cat}^{-1} s^{-1}	87 kJ mol^{-1}
Water Gas Shift (WGS) Eq. (9)	0.0248 m^4 mg_{cat}^{-1} s^{-1} mol^{-1}	86 kJ mol^{-1}
Methane Steam Reforming (MSR) Eq. (10)	0.0128 m^7 mg_{cat}^{-1} s^{-1} mol^{-2}	145 kJ mol^{-1}

Please cite this article as: Cifuentes A et al., Modelling of the ethanol steam reforming over Rh-Pd/CeO_2 catalytic wall reactors, International Journal of Hydrogen Energy, https://doi.org/10.1016/j.ijhydene.2019.11.034

Table 2 – Activation energy for reactions involved in ESR.

Reference	Catalyst	Ea (kJ mol^{-1}) Ethanol decomposition Eq. (5)	Ea (kJ mol^{-1}) Water gas shift Eq. (6)	Ea (kJ mol^{-1}) Methane steam reforming Eq. (7)
This work	Rh-Pd/CeO_2	87	86	145
[13]	Rh-Pd/CeO_2	87	70	156
[18]	Co3O4/ZnO	130	70	–
[31]	Rh/MgAl2O4/Al2O3	86	151	107[b]
[34]	Rh/MgAl2O4/Al2O3	303	56	188[b]
[35]	Pt-Co/CeO_2-SiO_2	28	60	232[b]
[35]	Ni-Co/CeO_2-SiO_2	24	35	77[b]
[36]	Pd/Al_2O_3	148[a]	60	107[b]

[a] $C_2H_5OH(g) + H_2O(g) \rightarrow CH_4(g) + CO_2(g) + 2H_2(g)$.
[b] $CH_4(g) + H_2O(g) \rightarrow CO(g) + 3H_2(g)$.

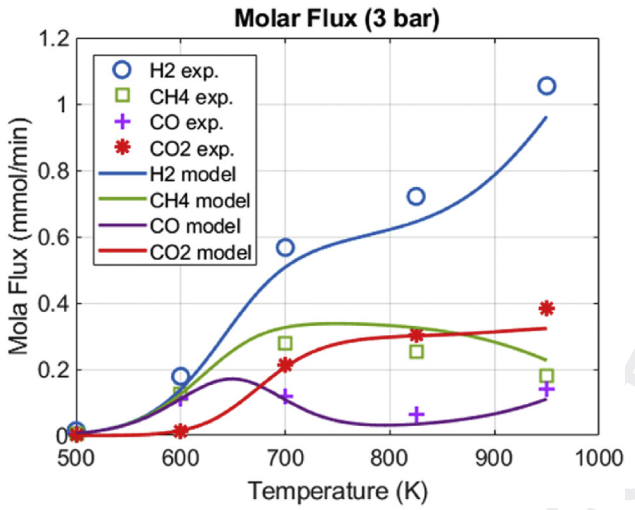

Fig. 3 – Exit molar fluxes for different operational temperatures of H_2, CH_4, CO and CO_2. P = 3 bar, S/C = 3, W/F = 7.58 10^{-2} kg h L_{liq}^{-1}.

$$X_{EtOH} = \frac{F_{C_2H_5OH,in} - F_{C_2H_5OH,out}}{F_{C_2H_5OH,in}} \quad (13)$$

where $F_{C_2H_5OH,in}$ and $F_{C_2H_5OH,out}$ are the inlet and outlet ethanol molar fluxes, respectively.

- Hydrogen yield (%):

$$\eta = \frac{F_{H_2}}{6 \cdot F_{C_2H_5OH,in}} 100 \quad (14)$$

where F_{H_2} is the outlet hydrogen molar flux.

Mesh

A mesh independency study was carried out to determine the optimal mesh number with the minimum computational cost. The simulations conditions were 6 bar, 700 K, S/C = 3, and a liquid load of 55 μLliq/min. The results obtained of the ethanol conversion versus the number of mesh elements are shown in Fig. 2. By increasing from 12,611 elements to 14,144, the

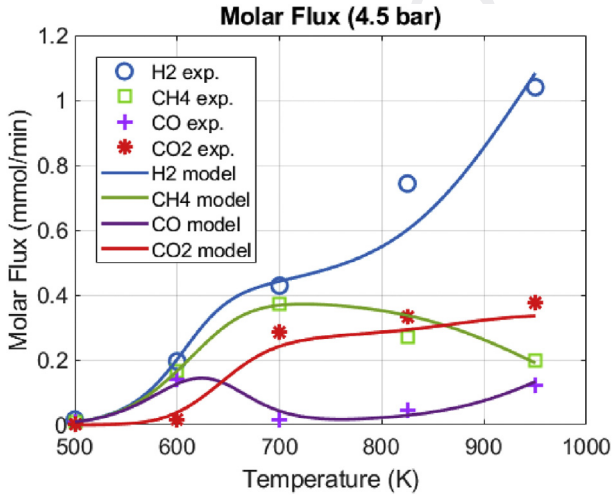

Fig. 4 – Exit molar fluxes for different operational temperatures of H_2, CH_4, CO and CO_2. P = 4.5 bar, S/C = 3, W/F = 7.58 10^{-2} kg h L_{liq}^{-1}.

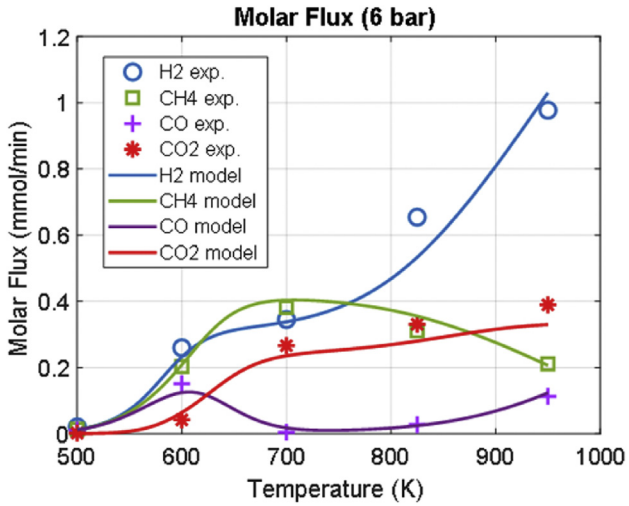

Fig. 5 – Exit molar fluxes for different operational temperatures of H_2, CH_4, CO and CO_2. P = 6 bar, S/C = 3, W/F = 7.58 10^{-2} kg h L_{liq}^{-1}.

Please cite this article as: Cifuentes A et al., Modelling of the ethanol steam reforming over Rh-Pd/CeO_2 catalytic wall reactors, International Journal of Hydrogen Energy, https://doi.org/10.1016/j.ijhydene.2019.11.034

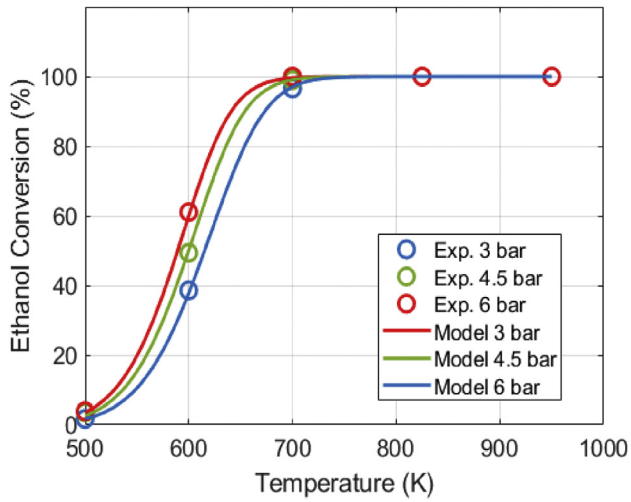

Fig. 6 – Ethanol conversion for different pressure and temperature conditions. S/C = 3, W/F = 7.58 10^{-2} kg h L_{liq}^{-1}.

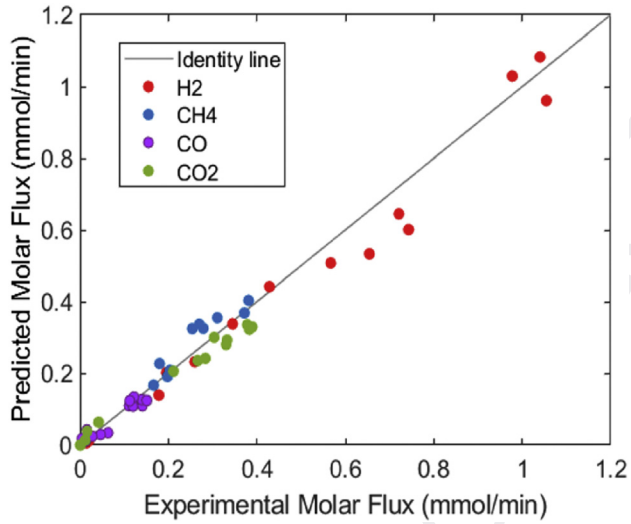

Fig. 7 – Parity plot for calculated vs. experimental exit molar flowrates for different pressure and temperature conditions. S/C = 3, W/F = 7.58 10^{-2} kg h L_{liq}^{-1}.

ethanol conversion difference was only 0.02%. Therefore, increasing the mesh elements had a negligible difference. Accordingly, this solution (12,611 elements) becomes independent from the mesh number and it was used for all subsequent computational studies.

Results and discussion

Table 1 shows the parameters for each reaction that have been estimated in order to obtain the best fitting values with the least squares method. These values compare well with those reported in the literature, as shown in Table 2, where the activation energy values reported for the three reactions involved in the ESR are compiled. The estimated activation energy values of this work are within the range of those reported experimentally.

To validate and evaluate the reliability of the model, the computational results were contrasted with experimental data in terms of molar fluxes of H_2, CO, CO_2 and CH_4 as well as ethanol conversion values [13]. As seen in Figs. 3–5, there is a good agreement between the computed results and experimental outlet molar fluxes, not only in the values but also in the trends. In addition, ethanol conversion (Eq. (13)) fits well with the experimental data at different pressures and temperatures (Fig. 6). A parity plot of experimental vs. calculated molar flux values is shown in Fig. 7 (R^2 = 0.977). However, model validation is only guaranteed in the range of 500–950 K, 3–6 bar and S/C = 3; simulations performed outside this range are not contrasted with experimental data.

Concerning the temperature distribution of the catalytic honeycomb under ESR conditions, Fig. 8 shows a 3D view at two different temperatures, 750 and 950 K, at 3 bar. As expected, there is a decrease of temperature at the entrance of the honeycomb. This is ascribed to the endothermic character of the first step of the ESR process, which is the decomposition of ethanol (Eq. (5)). The decrease of temperature is more evident at the central part of the honeycomb due to the well-known heat transfer limitations of cordierite. A similar trend is obtained at 4.5 and 6 bar (not shown).

The simulated profile distribution of species along a single channel at the centre of the catalytic honeycomb at 950 K and 3 bar is shown in Fig. 9. Ethanol is completely transformed at the very beginning of the honeycomb (first 2 mm, approximately). However, the distribution of products does not correspond to the stoichiometry of the decomposition of ethanol (Eq. (5)), which nominally yields equal molar

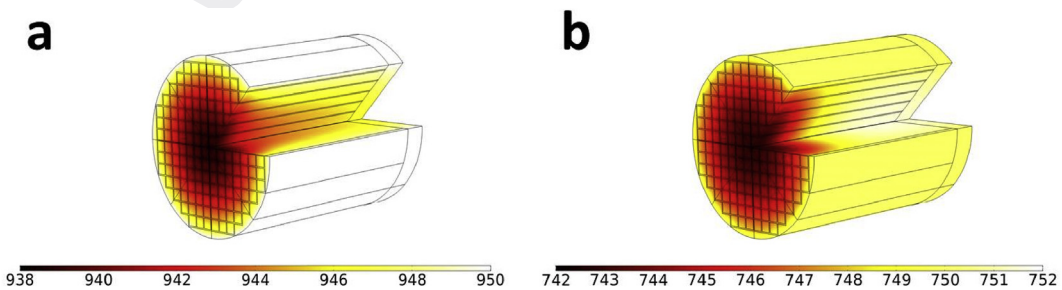

Fig. 8 – Temperature field (K) at P = 3 bar and external temperature of 950 K (a) and 750 K (b).

Please cite this article as: Cifuentes A et al., Modelling of the ethanol steam reforming over Rh-Pd/CeO_2 catalytic wall reactors, International Journal of Hydrogen Energy, https://doi.org/10.1016/j.ijhydene.2019.11.034

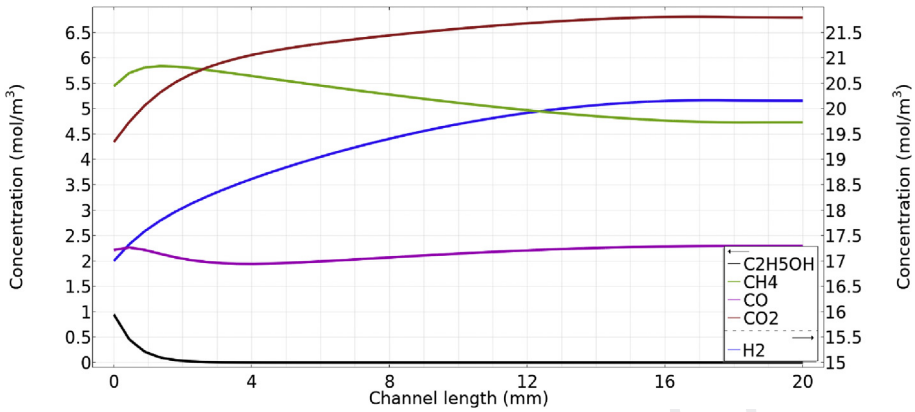

Fig. 9 – Molar concentration of different species vs. channel length. T = 950 K, P = 3 bar, S/C = 3, W/F = 7.58 10^{-2} kg h L_{liq}^{-1}.

concentrations between H_2, CO and CH_4. The presence of CO_2 and a high molar concentration of H_2 are indicative that the second step of the reaction, the water gas shift equilibrium (Eq. (6)), operates efficiently on the Rh-Pd/CeO_2 catalyst. As deduced from Fig. 9, this step is dominant shortly after the first millimetres of the honeycomb. The last stage of the ESR process, the steam reforming of methane (Eq. (7)), originated mostly from the initial decomposition of ethanol but also from methanation of carbon oxides with H_2, dominates most of the channel length. This is the reason why the molar concentration of both CO and CO_2 increase along the channel. The molar concentrations at the end of the channel approach those predicted by the thermodynamic equilibrium and larger lengths do not result in any additional advantage for the production of H_2 under these operation conditions.

Fig. 10 shows the ethanol conversion and hydrogen yield simulated for different space time values and temperatures. As expected, the ethanol conversion decreases progressively when the residence time decreases, being the decrease in ethanol conversion strongly related to the reaction temperature; the lower the temperature the stronger the ethanol conversion decay. The hydrogen yield follows the same trends, but given the different influence of space time and temperature on each reaction (ethanol decomposition, WGS and methane reforming), the trends exhibit different profiles and simulation appears as a valuable tool for predicting the hydrogen production.

Finally, the model has been used to explore the best operational conditions for producing hydrogen at S/C = 3 with the

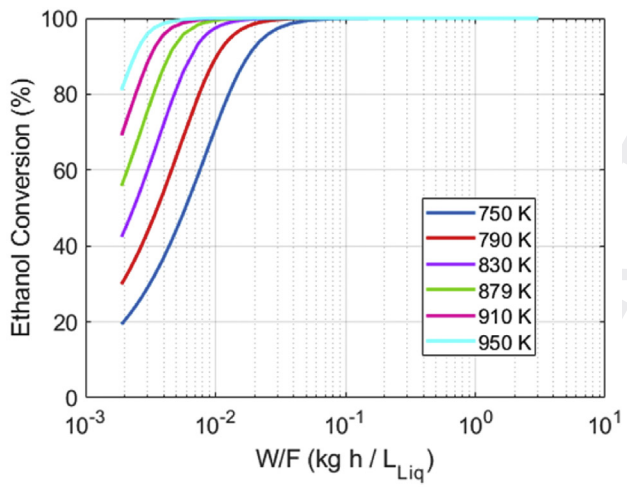

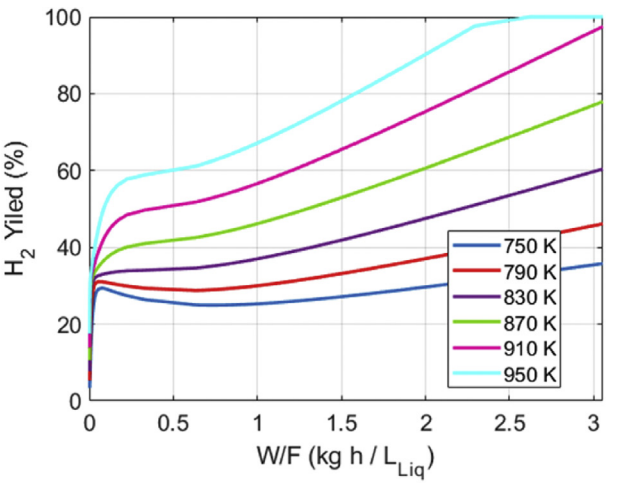

Fig. 10 – Ethanol conversion and hydrogen yield for different space time values and temperatures. P = 3 bar, S/C = 3.

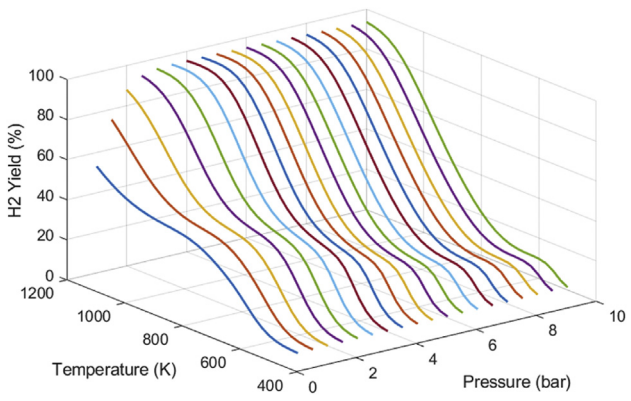

Fig. 11 – Hydrogen yield for different pressures and temperatures. S/C = 3, W/F = 7.58 10^{-2} kg h $Lliq^{-1}$.

Please cite this article as: Cifuentes A et al., Modelling of the ethanol steam reforming over Rh-Pd/CeO_2 catalytic wall reactors, International Journal of Hydrogen Energy, https://doi.org/10.1016/j.ijhydene.2019.11.034

catalytic honeycomb at a fixed space time. Fig. 11 shows the calculated H_2 yield, as defined in Eq. (14)., obtained at 500–1200 K and 1–10 bar. It is important to recall that the gas density and residence time of the reacting mixture increase with pressure, which has an influence on the hydrogen yield. This is particularly important at low pressure values (below ca. 2 bar). As anticipated, temperature has a positive effect on the ESR due to thermodynamics. However, the production of hydrogen at intermediate temperature (700–750 K) is hindered due to methanation, which is a reaction that consumes high amounts of H_2. This effect is more severe at high pressure, as expected from the stoichiometry of the reaction. At high temperature (ca. above 800 K), the production of hydrogen increases sharply and the maximum yield of hydrogen is obtained following the steam reforming of methane, which is favoured at low pressure values. A maximum yield of hydrogen around 80% is expected at a working temperature of about 1150 K and a pressure of about 4 bar.

Conclusions

A catalytic honeycomb consisting of a commercial cordierite 400 cpsi structure coated with Rh-Pd/CeO_2 has been modelled for the steam reforming of ethanol aimed to produce hydrogen at a steam to carbon ratio of S/C = 3. The model has been constructed and validated from experimental data available in the literature (ethanol conversion values and molar flow rates of products) recorded at different temperature and pressure. Three reactions have been considered in the model (ethanol decomposition, water gas shift and methane steam reforming). The kinetic parameters and activation energy values obtained from the model are within those reported in the literature. The model has been used to analyse in detail the heat transfer and the extent of the reactions that take place inside the catalytic honeycomb during the steam reforming of ethanol, where it is not feasible to acquire data. The optimal operation conditions (temperature and pressure) for the catalytic honeycomb have been determined at 1150 K and 4 bar, with a maximum hydrogen yield of 80%.

Acknowledgments

This work has been funded by projects MICINN/FEDER RTI2018-093996-B-C31 and GC 2017 SGR 128. AC is grateful to Generalitat de Catalunya and Addlink Software Científico S.L. for Industrial Doctorate grant 063/2018. JL is a Serra Húnter Fellow and is grateful to ICREA Academia program. We are grateful to Vicente Roda and Alejandro Martinez (EEBE) for technical assistance.

Nomenclature

ESR	ethanol steam reforming
WGS	water gas shift
MSR	methane steam reforming
S/C	steam to carbon
W/F	weight to flow (kg h L_{liq}^{-1})
u	velocity vector, m s^{-1}
p	pressure, Pa
I	identity matrix
n	normal vector
F	external forces applied to the fluid, N m^{-3}
C_p	heat capacity at constant pressure, J kg^{-1} K^{-1}
T	temperature, K
k_{con}	thermal conductivity W m^{-1} K^{-1}
Q	external heat source, W m^{-2}
Q_r	reaction heat source, W m^{-2}
D_i	diffusion coefficient, m^2 s^{-1}
c_i	concentration, mol m^{-3}
R_i	species surface rate, mol m^{-2} s^{-1}
R	reaction rate, mol m^{-2} s^{-1}
k	reaction rate constant, Eq. (5) m mg_{cat}^{-1} s^{-1}; Eq. (6) m^4 mg_{cat}^{-1} s^{-1} mol^{-1}; Eq. (7) m^7 mg_{cat}^{-1} s^{-1} mol^{-2}
k_∞	pre-exponential factor, Eq. (5) m mg_{cat}^{-1} s^{-1}; Eq. (6) m^4 mg_{cat}^{-1} s^{-1} mol^{-1}; Eq. (7) m^7 mg_{cat}^{-1} s^{-1} mol^{-2}
K	equilibrium constant
E_a	activation energy, kJ mol^{-1}
R	universal gas constant, J mol^{-1} K^{-1}
ΔG_r°	Gibbs free energy of reaction (including formation terms), J mol^{-1}
J	diffusive flux, mol m^{-2} s^{-1}
F	molar flow rate, mol min^{-1} or mmol min^{-1}
X_{EtOH}	ethanol conversion
mgcat	catalyst mass, mg

Greek letters

ρ_f	density, kg m^{-3}
μ	dynamic viscosity, Pa s
C_{total}	sum of all concentration species, mol m^{-3}
H	hydrogen yield

Superscripts

γ	stoichiometric coefficient
$^\circ$	standard condition

Subscripts

i	species i
j	reaction j
C_2H_5OH	ethanol
CO	carbon monoxide
CO_2	carbon dioxide
H_2O	water
H_2	hydrogen
CH_4	methane
0	inlet

REFERENCES

[1] Acar C, Dincer I. Review and evaluation of hydrogen production options for better environment. J Clean Prod 2019;218:835–49. https://doi.org/10.1016/J.JCLEPRO.2019.02.046.

[2] Dincer I, Acar C. Innovation in hydrogen production. Int J Hydrogen Energy 2017;42:14843–64. https://doi.org/10.1016/J.IJHYDENE.2017.04.107.

Please cite this article as: Cifuentes A et al., Modelling of the ethanol steam reforming over Rh-Pd/CeO_2 catalytic wall reactors, International Journal of Hydrogen Energy, https://doi.org/10.1016/j.ijhydene.2019.11.034

[3] Kolb G. Review: microstructured reactors for distributed and renewable production of fuels and electrical energy. Chem Eng Process Process Intensif 2013;65:1–44. https://doi.org/10.1016/J.CEP.2012.10.015.

[4] Sharma YC, Kumar A, Prasad R, Upadhyay SN. Ethanol steam reforming for hydrogen production: latest and effective catalyst modification strategies to minimize carbonaceous deactivation. Renew Sustain Energy Rev 2017;74:89–103. https://doi.org/10.1016/J.RSER.2017.02.049.

[5] Ni M, Leung DYC, Leung MKH. A review on reforming bio-ethanol for hydrogen production. Int J Hydrogen Energy 2007;32:3238–47. https://doi.org/10.1016/J.IJHYDENE.2007.04.038.

[6] Contreras JL, Salmones J, Colín-Luna JA, Nuño L, Quintana B, Córdova I, et al. Catalysts for H_2 production using the ethanol steam reforming (a review). Int J Hydrogen Energy 2014;39:18835–53. https://doi.org/10.1016/J.IJHYDENE.2014.08.072.

[7] Llorca J, Corberán VC, Divins NJ, Fraile RO, Taboada E. Hydrogen from bioethanol. Renew Hydrog Technol 2013:135–69. https://doi.org/10.1016/B978-0-444-56352-1.00007-6.

[8] Idriss H, Scott M, Llorca J, Chan SC, Chiu W, Sheng P-Y, et al. A phenomenological study of the metal–oxide interface: the role of catalysis in hydrogen production from renewable resources. ChemSusChem 2008;1:905–10. https://doi.org/10.1002/cssc.200800196.

[9] Divins NJ, Angurell I, Escudero C, Pérez-Dieste V, Llorca J. Influence of the support on surface rearrangements of bimetallic nanoparticles in real catalysts. Science 2014;346:620–3. https://doi.org/10.1126/science.1258106.

[10] Divins NJ, Llorca J. In situ photoelectron spectroscopy study of ethanol steam reforming over RhPd nanoparticles and RhPd/CeO_2. Appl Catal A Gen 2016;518:60–6. https://doi.org/10.1016/J.APCATA.2015.08.018.

[11] Divins NJ, Casanovas A, Xu W, Senanayake SD, Wiater D, Trovarelli A, et al. The influence of nano-architectured CeO_x supports in RhPd/CeO_2 for the catalytic ethanol steam reforming reaction. Catal Today 2015;253:99–105. https://doi.org/10.1016/J.CATTOD.2014.12.042.

[12] Soler L, Casanovas A, Ryan J, Angurell I, Escudero C, Pérez-Dieste V, et al. Dynamic reorganization of bimetallic nanoparticles under reaction depending on the support nanoshape: the case of RhPd over ceria nanocubes and nanorods under ethanol steam reforming. ACS Catal 2019;9:3641–7. https://doi.org/10.1021/acscatal.9b00463.

[13] López E, Divins NJ, Anzola A, Schbib S, Borio D, Llorca J. Ethanol steam reforming for hydrogen generation over structured catalysts. Int J Hydrogen Energy 2013;38:4418–28. https://doi.org/10.1016/J.IJHYDENE.2013.01.174.

[14] Casanovas A, Divins NJ, Rejas A, Bosch R, Llorca J. Finding a suitable catalyst for on-board ethanol reforming using exhaust heat from an internal combustion engine. Int J Hydrogen Energy 2017;42:13681–90. https://doi.org/10.1016/J.IJHYDENE.2016.11.197.

[15] López E, Divins NJ, Llorca J. Hydrogen production from ethanol over Pd–Rh/CeO_2 with a metallic membrane reactor. Catal Today 2012;193:145–50. https://doi.org/10.1016/J.CATTOD.2012.06.030.

[16] Koch R, López E, Divins NJ, Allué M, Jossen A, Riera J, et al. Ethanol catalytic membrane reformer for direct PEM FC feeding. Int J Hydrogen Energy 2013;38:5605–15. https://doi.org/10.1016/J.IJHYDENE.2013.02.107.

[17] Divins NJ, López E, Rodríguez Á, Vega D, Llorca J. Bio-ethanol steam reforming and autothermal reforming in 3-μm channels coated with RhPd/CeO_2 for hydrogen generation. Chem Eng Process Process Intensif 2013;64:31–7. https://doi.org/10.1016/J.CEP.2012.10.018.

[18] Uriz I, Arzamendi G, López E, Llorca J, Gandía LM. Computational fluid dynamics simulation of ethanol steam reforming in catalytic wall microchannels. Chem Eng J 2011;167:603–9. https://doi.org/10.1016/J.CEJ.2010.07.070.

[19] Rostami AA, Mujumdar AS, Saniei N. Flow and heat transfer for gas flowing in microchannels: a review. Heat Mass Transf 2002;38:359–67. https://doi.org/10.1007/s002310100247.

[20] Wang M, Lan X, Li Z. Analyses of gas flows in micro- and nanochannels. Int J Heat Mass Transf 2008;51:3630–41. https://doi.org/10.1016/J.IJHEATMASSTRANSFER.2007.10.011.

[21] Ma R, Castro-Dominguez B, Mardilovich IP, Dixon AG, Ma YH. Experimental and simulation studies of the production of renewable hydrogen through ethanol steam reforming in a large-scale catalytic membrane reactor. Chem Eng J 2016;303:302–13. https://doi.org/10.1016/J.CEJ.2016.06.021.

[22] Inbamrung P, Sornchamni T, Prapainainar C, Tungkamani S, Narataruksa P, Jovanovic GN. Modeling of a square channel monolith reactor for methane steam reforming. Energy 2018;152:383–400. https://doi.org/10.1016/J.ENERGY.2018.03.139.

[23] Sidhu TPK, Roy S. Optimal design of washcoated monolith catalyst for compact, heat-integrated ethanol reformers. Int J Hydrogen Energy 2019;44:11472–87. https://doi.org/10.1016/J.IJHYDENE.2019.03.129.

[24] Sidhu TPK, Govil A, Roy S. Optimal monolithic configuration for heat-integrated ethanol steam reformer. Int J Hydrogen Energy 2017;42:7770–85. https://doi.org/10.1016/J.IJHYDENE.2017.01.008.

[25] Dehkordi TK, Hormozi F, Jahangiri M. Using conical reactor to improve efficiency of ethanol steam reforming. Int J Hydrogen Energy 2016;41:17084–92. https://doi.org/10.1016/J.IJHYDENE.2016.07.040.

[26] Lee B, Yun S-W, Kim S, Heo J, Kim Y-T, Lee S, et al. CO_2 reforming of methane for H_2 production in a membrane reactor as CO_2 utilization: computational fluid dynamics studies with a reactor geometry. Int J Hydrogen Energy 2019;44:2298–311. https://doi.org/10.1016/J.IJHYDENE.2018.09.184.

[27] Gallucci F, Van Sint Annaland M, Kuipers JAM. Pure hydrogen production via autothermal reforming of ethanol in a fluidized bed membrane reactor: a simulation study. Int J Hydrogen Energy 2010;35:1659–68. https://doi.org/10.1016/J.IJHYDENE.2009.12.014.

[28] Ghasemzadeh K, Ghahremani M, Amiri TY, Basile A. Performance evaluation of PdAg membrane reactor in glycerol steam reforming process: development of the CFD model. Int J Hydrogen Energy 2019;44:1000–9. https://doi.org/10.1016/J.IJHYDENE.2018.11.086.

[29] Irani M, Alizadehdakhel A, Pour AN, Hoseini N, Adinehnia M. CFD modeling of hydrogen production using steam reforming of methane in monolith reactors: surface or volume-base reaction model? Int J Hydrogen Energy 2011;36:15602–10. https://doi.org/10.1016/J.IJHYDENE.2011.09.030.

[30] Ghasemzadeh K, Andalib E, Basile A. Evaluation of dense Pd–Ag membrane reactor performance during methanol steam reforming in comparison with autothermal reforming using CFD analysis. Int J Hydrogen Energy 2016;41:8745–54. https://doi.org/10.1016/J.IJHYDENE.2015.11.139.

[31] Graschinsky C, Laborde M, Amadeo N, Le Valant A, Bion N, Epron F, et al. Ethanol steam reforming over Rh(1%)$MgAl_2O_4$/Al_2O_3: a kinetic study. Ind Eng Chem Res 2010;49:12383–9. https://doi.org/10.1021/ie101284k.

[32] Xu J, Froment GF. Methane steam reforming, methanation and water-gas shift: I. Intrinsic kinetics. AIChE J 1989;35:88–96. https://doi.org/10.1002/aic.690350109.

[33] Chemical-kinetic mechanisms for combustion applications, mechanical and aerospace engineering. UC San Diego, http://

Please cite this article as: Cifuentes A et al., Modelling of the ethanol steam reforming over Rh-Pd/CeO_2 catalytic wall reactors, International Journal of Hydrogen Energy, https://doi.org/10.1016/j.ijhydene.2019.11.034

web.eng.ucsd.edu/mae/groups/combustion/index.html. [Accessed 22 July 2019].
[34] Rossetti I, Compagnoni M, Torli M. Process simulation and optimization of H_2 production from ethanol steam reforming and its use in fuel cells. 2. Process analysis and optimization. Chem Eng J 2015;281:1036–44. https://doi.org/10.1016/J.CEJ.2015.08.045.
[35] Ruocco C, Palma V, Ricca A. Experimental and kinetic study of oxidative steam reforming of ethanol over fresh and spent bimetallic catalysts. Chem Eng J 2018:119778. https://doi.org/10.1016/J.CEJ.2018.08.164.
[36] Izurieta EM, Borio DO, Pedernera MN, López E. Parallel plates reactor simulation: ethanol steam reforming thermally coupled with ethanol combustion. Int J Hydrogen Energy 2017;42:18794–804. https://doi.org/10.1016/J.IJHYDENE.2017.06.134.

Please cite this article as: Cifuentes A et al., Modelling of the ethanol steam reforming over Rh-Pd/CeO_2 catalytic wall reactors, International Journal of Hydrogen Energy, https://doi.org/10.1016/j.ijhydene.2019.11.034